Research Square

Preprints are preliminary reports that have not undergone peer review.
They should not be considered conclusive, used to inform clinical practice,
or referenced by the media as validated information.

Groundwater Detection Using Geophysical Methods in Different Overburden Types in the Karst Region of Southwest China

Zhijie Zheng
Institute of Karst Geology, Chinese Academy of Geological Sciences /Key Laboratory of Karst Dynamics, MNR & GZAR/International Research Center on Karst under the Auspices of UNESCO

Jie Zeng
5225943810qq.com

Institute of Karst Geology, Chinese Academy of Geological Sciences /Key Laboratory of Karst Dynamics, MNR & GZAR/International Research Center on Karst under the Auspices of UNESCO

Jiayong Yan
SinoProbe Laboratory Chinese Academy of Geological Sciences

Fuping Gan
Institute of Karst Geology, Chinese Academy of Geological Sciences /Key Laboratory of Karst Dynamics, MNR & GZAR/International Research Center on Karst under the Auspices of UNESCO

Xiuhua Lu
Institute of Karst Geology, Chinese Academy of Geological Sciences /Key Laboratory of Karst Dynamics, MNR & GZAR/International Research Center on Karst under the Auspices of UNESCO

Research Article

Keywords: Overburden, Exposed type, Covered type, Buried type, Groundwater detection, Geophysics

Posted Date: November 9th, 2026

DOI: https://doi.org/10.21203/rs.3.rs-11323960/v1

License: This work is licensed under a Creative Commons Attribution 4.0 International License.
Read Full License

Additional Declarations: No competing interests reported.

Groundwater Detection Using Geophysical Methods in Different Overburden Types in the Karst Region of Southwest China

Zhijie Zheng [1, 2, 3], Jie Zeng [1, 3], Jiayong Yan[4*], Fuping Gan [1, 3], Xiuhua Lu [1, 3]

1. Institute of Karst Geology, Chinese Academy of Geological Sciences /Key Laboratory of Karst Dynamics, MNR & GZAR/International Research Center on Karst under the Auspices of UNESCO, Guilin, Guangxi, China；2. School of Resources and Environmental Engineering, Hefei University of Technology, Hefei, Anhui, China；3. Pingguo Guangxi, Karst Ecosystem, National Observation and Research Station, Pingguo, Guangxi, China; 4. SinoProbe Laboratory，Chinese Academy of Geological Sciences , Beijing, China

*Corresponding author: Jie Zeng , Email: 522594381@qq.com

Abstract The overburden has a decisive influence on geophysical groundwater detection. (1) Exposed type area: The soluble rock aquifer is directly exposed at the surface. For conventional direct current (DC) electrical methods, this layer exhibits high resistivity, which hinders the application of the DC resistivity method. Non-ground-contact geophysical methods such as ground-penetrating radar (GPR) and transient electromagnetic (TEM) methods are often used for groundwater detection in such areas. (2) Covered type area: The soluble rock aquifer is overlain by clay, sand, gravel, and other materials, which forms an electrical layer with resistivity ranging from tens to hundreds of Ω·m. When the overburden thickness is less than 30 m, the conventional resistivity method is suitable for groundwater detection; when the overburden thickness exceeds 30 m, methods such as audio-frequency magnetotellurics (AMT), controlled-source audio-frequency magnetotellurics (CSAMT), or TEM are recommended. (3) Buried type area: The soluble rock is overlain by clastic rocks, which generally have resistivity ranging from tens to

*Corresponding author: Jie Zeng, Email: 522594381@qq.com

hundreds of Ω·m. For relatively intact, slightly weathered basalt, the resistivity can be on the order of $n\times10^3$–$n\times10^4$ Ω·m. When the groundwater level is shallow, electromagnetic methods are preferable. When the groundwater level is deep, the conventional resistivity method can be used within the target detection depth range. However, under confined site conditions and with deep target bodies, methods such as AMT, CSAMT, or TEM should be used for groundwater detection. Other methods may be integrated when geophysical anomalies are ambiguous or multiple interpretations are available to ensure comprehensive interpretation.

Keywords Overburden; Exposed type; Covered type; Buried type; Groundwater detection; Geophysics

1 Introduction

Groundwater, as a globally strategic water resource, supports the production and domestic water needs of billions of people; it plays an irreplaceable role in ensuring security in urban and rural water supply and maintaining ecosystem balance (Alao et al. 2025). However, under the dual pressures of intensified climate change and increased human activities, the spatiotemporal distribution pattern of regional water resources has changed considerably. The increased frequency and intensity of droughts have posed unprecedented challenges to groundwater systems (Fokker et al. 2024). In the current resource and environment context, accurately detecting groundwater resources and scientifically evaluating aquifer water abundance have become core issues in hydrogeology and geophysics.

The occurrence conditions of groundwater are controlled by complex geological structures and lithological assemblages, among which the spatial relationship between the overburden and the aquifer has a decisive influence on groundwater detection. Based on differences in the contact

relationship between overburden and aquifer and hydrogeological characteristics, groundwater systems can be divided into three basic types: exposed type, where the aquifer is directly exposed at the surface without a continuous overburden barrier; covered type, where a certain thickness of unconsolidated sediments or weathered residual layers exists above the aquifer, with discontinuous or weakly permeable contact between them; and buried type, where the aquifer is completely sealed by a regional aquiclude with no direct hydraulic connection to the surface (Wang 2003; Chen 1988). This classification system not only serves as the basic framework for regional hydrogeological surveys but also provides an important geological basis for selecting groundwater detection methods (Wang 2002).

Different overburden types impose differentiated requirements on the technical approaches of geophysical methods. In exposed type areas, the aquifer is directly exposed, and surface karst features or structural fissures can be directly identified through geological surveys. Traditional hydrogeological mapping combined with geophysical methods can often effectively delineate groundwater enrichment zones (Wang et al. 2025; Wang et al. 2022). Wang et al. (2021) used geophysical exploration, hydrogeological surveys, and drilling to reveal the characteristics of karst development and the vertical stratification of groundwater distribution in the exposed dolomite area. In covered and buried type areas, the barrier of the overburden conceals aquifer information underground, which causes difficulty for conventional ground surveys to directly obtain the spatial distribution and hydraulic properties of the aquifer. Therefore, geophysical detection techniques must be used to achieve indirect interpretation of the subsurface structure (Qi et al. 2021; Pan et al. 2015). Cao et al. (2018) highlighted that combining hydrogeological surveys with geophysics can

significantly improve the success rate of locating water wells in karst areas, and the AMT method provides reliable interpretation results under conditions of shallow overburden and deep groundwater. Guo et al. (2022) proposed that buried type areas are dominated by paleokarst, with a single target aquifer and deep and extremely uneven development. The combination of electrical resistivity tomography (ERT), composite profiling, and induced polarization sounding achieved a water exploration success rate of 86.67%. Geophysical methods have shown unique value in characterizing overburden structure; their sensitivity to differences in physical fields of strata enabled identification of concealed aquifers and description of water-rich targets (Li et al. 2022; Wang et al. 2025).

In recent years, geophysical detection techniques have greatly progressed in the field of groundwater exploration. Among them, resistivity and electromagnetic methods are the most widely used. The direct current (DC) resistivity method identifies aquifer locations by detecting stratigraphic electrical differences. ERT can finely characterize shallow overburden structure and aquifer spatial morphology (Subramani et al. 2024; Zheng et al. 2019; Zheng et al. 2024). Electromagnetic methods, especially AMT, have advantages in revealing deep aquifer interfaces and structural fracture zones (Rulff et al. 2025; Zheng et al. 2025; Bon et al. 2022). Magnetic methods are mainly used to detect basement structures, faults, and lithological boundaries, which indirectly indicates groundwater occurrence environments (Gabriel et al. 2025). Seismic exploration reflects stratigraphic mechanical properties through wave velocity differences, which provides important constraints for identifying aquifer boundaries (Wang et al. 2025; Alao et al. 2025). Breakthroughs in seismic wave velocity monitoring methods have enabled continuous

tracking of water dynamics in saturated and unsaturated zones (Fokker et al. 2024). The microtremor Horizontal-to-Vertical Spectral Ratio (HVSR) method is mainly used to identify the location and water content of karst fissures and conduits (Liang et al. 2020; Liu et al. 2019). The development of nuclear magnetic resonance methods has enabled direct evaluation of aquifer water abundance (Wang et al. 2025; Sun et al. 2012). Radioactive methods use soil radon values to determine fault locations, which indirectly provides a basis for groundwater detection (Huang et al. 2022; Liao et al. 2017). In addition, the recently introduced seismoelectric imaging method utilizes the electromagnetic field excited when seismic waves pass through the subsurface medium (seismoelectric effect) to directly detect aquifer interfaces. By performing seismic migration processing on seismoelectric signals, imaging of aquifer interfaces is achieved (Liu et al. 2024; Sun et al. 2025). Research shows that combining corresponding geophysical methods for different overburden types can significantly improve the success rate of water exploration (Wang et al. 2025).

However, existing research mostly focuses on case studies of a single overburden type or specific geophysical methods. Systematic comparisons of the applicability, technical combination strategies, and interpretation logic of geophysical methods under different overburden conditions are still relatively weak (Wang et al. 2025; Zohdy et al. 1974). The following questions remain unanswered: How do the lithological structure, thickness variation, and hydrogeological properties of different overburden types affect the response characteristics of various geophysical methods? How can groundwater be detected economically, quickly, and accurately in different types of overburden areas in the karst rocky mountain region of Southwest China? How can differentiated

geophysical technology sequences be constructed and optimal method combinations selected? These issues directly relate to the scientificity and effectiveness of groundwater detection in complex overburden areas and are urgently needed to be addressed.

Based on the aforementioned discussion, this study systematically reviews the classification of overburden types and their hydrogeological characteristics, along with the technical principles and applicable conditions of major geophysical detection methods. It focuses on analyzing the method combinations and application cases for groundwater detection in different types of overburden areas. Then, it discusses the technical optimization paths of geophysical methods under overburden constraints. This study provides theoretical reference and methodological support for groundwater resource exploration under complex geological conditions.

2 Study Areas

2.1 Exposed Type Areas

In exposed type areas, the aquifer or its overlying rock is directly exposed at the surface without continuous coverage of unconsolidated sediments (e.g., soil and clay). Atmospheric precipitation directly infiltrates through rock fissures, with high recharge efficiency but significant seasonal influence. An unsaturated zone of varying thickness exists between the surface and the water table, with water movement mainly vertical. Groundwater distribution is extremely uneven (Wang 2002), which is mainly stored in fissures and karst conduits, with strong anisotropy. Therefore, the

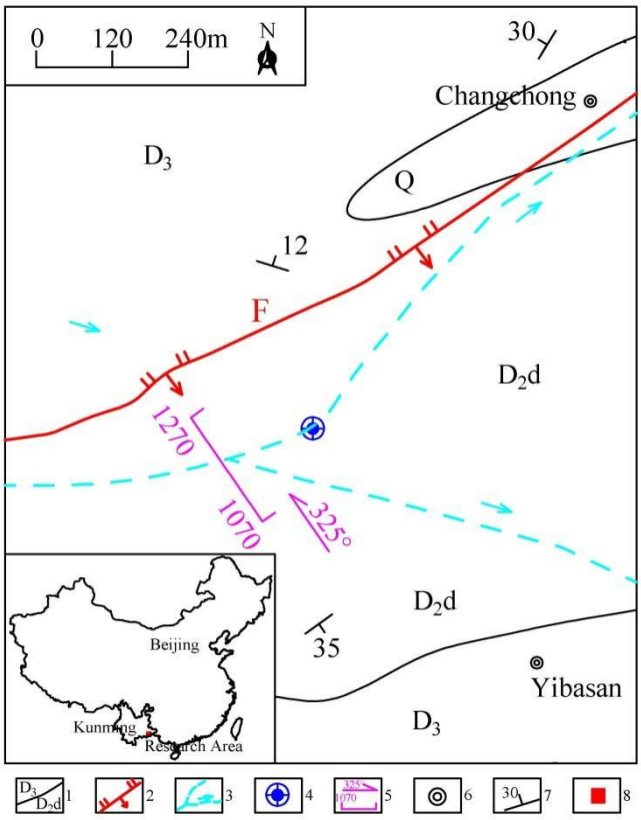
direction for water exploration mainly targets karst fissures and karst conduits.

For exposed rocks such as limestone and dolomite, the resistivity is generally very high, which reaches $n\times10^4$–$n\times10^5$ Ω·m. For conventional DC electrical methods, this section appears as a high resistivity layer, which prevents current penetration and forms an insulating shield. In addition, in exposed areas, the surface is mostly without unconsolidated sediment cover, which results in poor electrode-to-ground coupling. This condition is unfavorable for the application of DC resistivity methods. However, for electromagnetic methods, especially non-grounded ground-penetrating radar (GPR) and transient electromagnetic (TEM) methods, good application results can be achieved. Geophysical methods often use non-grounded electromagnetic methods. The Yibasan Village, Maguan County, Wenshan Prefecture, Yunnan Province, is taken as an example for analysis.

The study area is located in Pojiao Town, Maguan County, Wenshan Prefecture, Yunnan Province. The main landform types are karst landforms such as peak cluster depressions and peak cluster sinkholes, as well as structurally eroded medium mountain landforms. Surface karst features mainly include caves, underground rivers, sinkholes, depressions, swallets, solution wells, windows, karst peaks, and karst hills. The topographic relief is large, with elevations in the area generally ranging from 870 m to 1,800 m, relative height differences mostly exceeding 300 m, and terrain slopes generally greater than 30°.

The exposed strata in the study area are mainly the Middle Devonian Donggangling Formation

154 (D_2d), with gray to dark gray medium to massive cryptocrystalline and fine-grained limestone
155 interbedded with dolomite, and the Upper Devonian (D_3), with gray, dark gray medium to
156 thick-bedded limestone interbedded with argillaceous limestone and oolitic limestone, which are
157 locally interbedded with dolomite. Most of the study area has exposed bedrock, with only sporadic
158 Quaternary (Q) clay, silty clay mixed with weathered residual rock breccia and fragments covering
159 the northeast.
160
161 Groundwater in the study area is mainly classified into karst water, bedrock fissure water, and pore
162 water. Groundwater receives vertical and lateral recharge, as well as surface water infiltration
163 recharge. Discharge in the runoff zone is mainly through dissolution conduits and dissolution
164 fissures. Discharge volume is significantly and rapidly affected by rainfall, which results in
165 unstable groundwater levels and large dynamic changes. Preliminary hydrogeological surveys
166 indicate that a “Y”-shaped underground river system develops in the study area (Figure 1). The
167 system branches at a node into northeast and northwest trending underground rivers. Atmospheric
168 precipitation in the survey area directly flows into underground channels through sinkholes,
169 depressions, dissolution fissures, windows, and swallets, which converge into large springs and
170 underground rivers. The general groundwater flow direction is northwest-southeast. The main
171 geological structure in the study area is a circular shear structural system, with a
172 northeast-southwest trending reverse fault developed in the north. The rock mass has
173 well-developed joints and fissures.



174

175 **Fig. 1** Hydrogeological map of Yibasan Village, Yunnan Province

176 1- stratum code and stratum boundary 2- reverse fault 3- underground river and flow direction 4- karst window 5-

177 geophysical prospecting line and orientation 6- town and village location 7- stratum attitude 8- research area

178

179 **2.2 Covered Type Areas**

180

181 The presence of sediments such as clay, coarse sand, and gravel (thickness from a few meters to

182 tens of meters) overlying soluble rocks is a common overburden type in karst areas. Recharge can

183 occur vertically through the pores of the overburden or through surface water. Owing to the weak

184 permeability of the overburden, the underlying karst aquifer often exhibits slight confined

185 conditions (Pei et al. 2008).

186

The presence of the overburden causes the overall surface resistivity to be neither too high to prevent power supply nor too low to cause skin effect affecting exploration depth. This overburden type is the most suitable condition for conventional ground geophysical methods such as DC resistivity and induced polarization methods. However, when the site is narrow or the overburden is thick (greater than 30 m, Wang 2002), on the one hand, arranging a long profile to achieve greater exploration depth is difficult; on the other hand, the resolution of resistivity methods decreases. Therefore, under such conditions, electromagnetic methods are also recommended.

2.2.1 Thin Covered Type Areas

The overburden is generally less than 30 m (Wang 2002). The Sanwan Village, Matian Township, Yizhang County, Hunan Province, is taken as an example for analysis.

The study area is located in Matian Township, Yizhang County, Hunan Province. The landform is hilly valley, with a relative height difference of approximately 80 m between the valley and the surrounding mountains. The terrain within the valley is gently undulating. The overburden is yellowish-brown clay, with rice cultivation and relatively dense vegetation.

The main exposed stratum in the study area is the Triassic Daye Formation (Td). It consists of gray-black, medium to thick-bedded limestone, which is the main aquifer in the study area. An east-west trending fault develops in the study area.

The groundwater recharge source in the study area is atmospheric precipitation. Groundwater runoff and discharge are controlled by the east-west trending fault. Two descending springs develop in the north near the village entrance. The spring discharge is significantly affected by rainfall, with dry season cessation. The survey area has a large recharge area and relatively abundant groundwater (Figure 2).

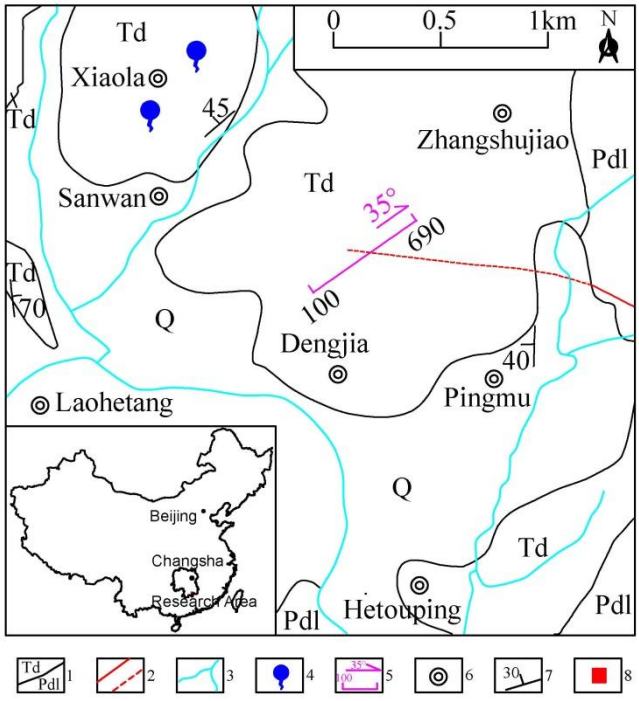


Fig. 2 Hydrogeological map of Sanwan Village, Hunan Province

1- stratum code and stratum boundary 2- measured fault and inferred fault 3- river 4- depression spring 5- geophysical prospecting line and orientation 6- town and village location 7- stratum attitude 8- research area

2.2.2 Thick Covered Type Areas

The overburden is generally greater than 30 m (Wang 2002). The Hongdong Village, Housuo Town, Fuyuan County, Yunnan Province, is taken as an example for analysis.

The landform of Fuyuan County comprises medium mountains with prominent canyon features, which are characterized by longitudinal river incision, fragmented terrain, high mountains and deep valleys, steep slopes and rapid currents, karst development, narrow river terraces, and scattered cultivated land. The study area is located on the northeast side of Hongdong Village, Housuo Town, Fuyuan County, Yunnan Province, with a karst depression landform consisting of gentle valley bottom terrain and steep valley slopes.

The main exposed strata in the study area are as follows: (1) Quaternary (Q): yellow, brownish-yellow clay. (2) Maokou Formation (P_1m): gray to light gray medium-thick massive limestone rich in dolomite and chert nodules. (3) Liangshan Formation (P_1l): light gray thin to medium-thick quartz sandstone and mudstone. (4) Qixia Formation (P_1q): gray to dark gray medium-thick limestone and chert nodule limestone, with occasional thin mudstone or marl interbeds at the lower part. The Maokou Formation (P_1m) is the main aquifer in the study area. No obvious structural features are developed in the study area.

The groundwater recharge source in the study area is atmospheric precipitation, with an overall flow direction from southwest to northeast. Rainwater infiltrates and recharges through karst fissures. Groundwater discharges to an outlet through an underground river near the area. The catchment area is moderate, which suggests relatively abundant underground water storage. A descending spring is exposed on the southwest side of the study area (Figure 3).

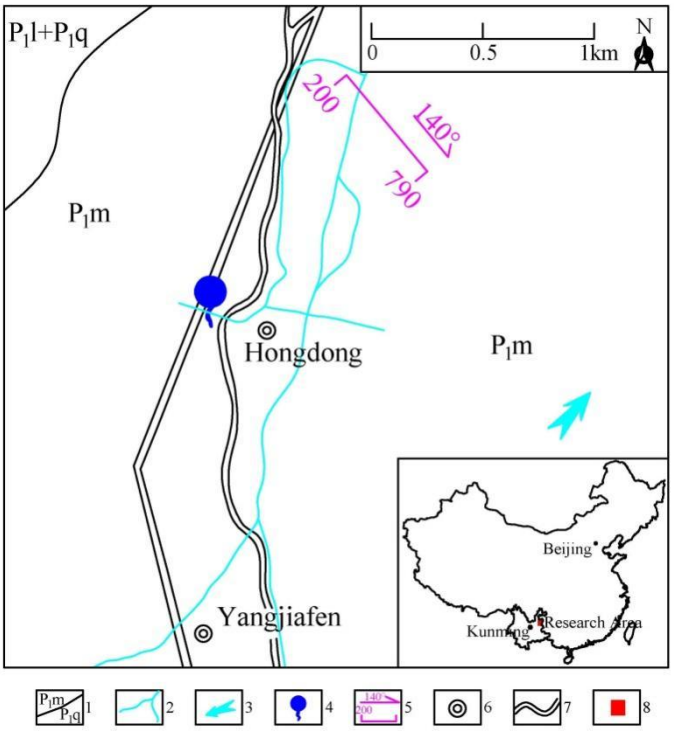


Fig. 3 Hydrogeological map of Hongdong Village, Yunnan Province

1- stratum code and stratum boundary 2- river 3- groundwater flow direction 4- depression spring 5- geophysical prospecting line and orientation 6- town and village location 7- road 8- research area

2.3 Buried Type Areas

This area refers to soluble rocks deeply buried underground (tens to hundreds of meters) by thick and continuous non-soluble rock layers, with no surface exposure. Local precipitation cannot directly recharge the soluble rock aquifer; it mainly depends on long-distance lateral runoff or leakage recharge from overlying aquifers. Groundwater exhibits obvious confined conditions (e.g., artesian wells), with long flow paths, deep circulation, and extremely slow renewal rates (Laskow et al. 2011).

Common non-soluble rock layers in the karst region of Southwest China are mainly clastic rocks, including Jurassic and Cretaceous red beds (red silty rock, sandstone, locally interbedded with limestone fragments), Permian Emeishan basalt, and sandstone or shale from other formations. A clastic rock caprock of a certain thickness generally has its own independent groundwater level and no hydraulic connection with the underlying soluble rock; the clastic rock layer is the target aquifer for water exploration. The resistivity of this clastic rock layer is generally between tens and hundreds of Ω·m. For relatively intact, slightly weathered basalt, the resistivity can reach $n\times10^3$–$n\times10^4$ Ω·m.

This study only discusses situations where the clastic rock caprock above soluble rocks is relatively thick. When the clastic rock is thin, groundwater detection can refer to the covered type area.

2.3.1 Shallow Buried Type Areas

When the groundwater level is shallow, the surface clastic rocks are often completely to strongly weathered, with large voids, and are water-bearing or saturated, with low resistivity. This area forms a good conductive shield for conventional resistivity methods, which greatly reduces the exploration depth. As a result, conventional resistivity methods are generally unfavorable, and electromagnetic methods are recommended. The Dalubian Village, Lefeng Township, Xuanwei City, Yunnan Province, is taken as an example for analysis.

The study area is located in Lefeng Township, Xuanwei City, Yunnan Province, which belongs to the Beipanjiang River basin. The terrain is generally high in the south and low in the north. The landform combination type is eroded medium mountain trough valley, with large topographic relief and relative height differences of 150–250 m.

The exposed strata in the study area are the Lower Triassic Feixianguan Formation (T_1f), which consists of gray-green, purplish-red silty mudstone, mudstone, sandstone interbedded with limestone and marl. The strata dip south-southeast at an angle of 15°–20°. Structurally, it is located on the northwest wing of the Tianba syncline, which is approximately 1 km from the core. The syncline axis trends 40°–70°, with the core consisting of Lower Triassic Feixianguan Formation (T_1f) strata and the two wings consisting of Carboniferous (C) to Permian (P) strata (Figure 7). The main water-bearing rock formation in the study area is the Lower Triassic Feixianguan Formation (T_1f), which is characterized by gray-green, purplish-red silty mudstone, mudstone, and sandstone, with fissures as the main water-bearing medium. This fissure aquifer is dominated by non-soluble hard brittle rock layers in clastic rocks, igneous rocks, and metamorphic rocks. Interlayer fissure aquifers, fault water-bearing zones, and weathered fissure aquifers are widespread. The burial and distribution of fissure water are more clearly controlled by bedding planes, the combination of different lithological strata, and geological structures. This fissure aquifer is distributed throughout Yunnan Province, with an exposed area of 26.38×10^4 km². This exposed area accounts for 66.95% of the total area of the province and is typical and representative. A northwest-southeast trending fault develops in the study area.

After atmospheric precipitation infiltrates and recharges groundwater along well-developed

fissures and joints, it flows from south to north and accumulates in the trough valley. The study area is located near the core of the Tianba syncline, with well-developed fissures and joints, which provide large groundwater storage space (Figure 4).

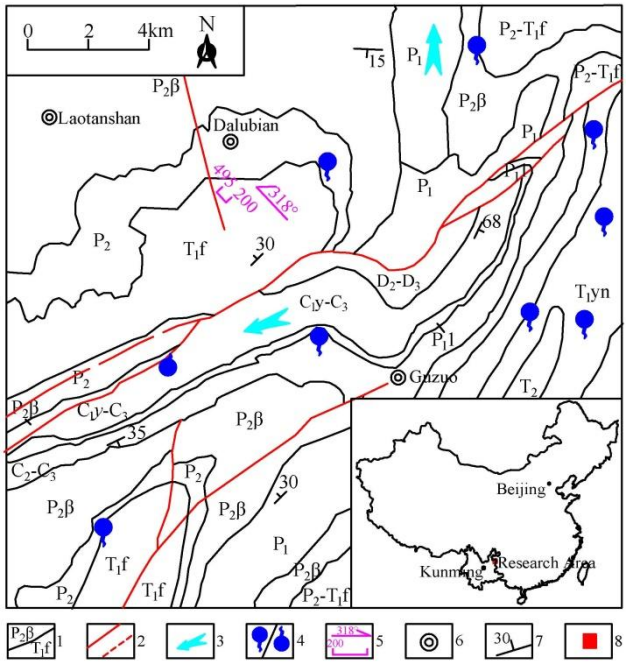


Fig. 4 Hydrogeological map of Dalubian Village, Yunnan Province

1- stratum code and stratum boundary 2- measured fault and inferred fault 3- groundwater flow direction 4- depression and ascending spring 5- geophysical prospecting line and orientation 6- town and village location 7- stratum attitude 8- research area

2.3.2 Deep Buried Type Areas

When the groundwater level is deep, the shallow resistivity is relatively high. Depending on site conditions, conventional resistivity methods can be used within the target detection depth range. However, when site conditions are narrow and the target is deep, electromagnetic methods (AMT, CSAMT, or TEM methods) are recommended for exploration. The Baiao Village, Tangtang Town,

Xuanwei City, Yunnan Province, is taken as an example for analysis.

In the study area, the overall terrain is high in the southwest and low in the northeast. The landform combination type is eroded medium mountain trough valley, with large topographic relief and relative height differences of 200–400 m.

The exposed strata on the hillsides are the Lower Triassic Feixianguan Formation (T_1f), with purplish-red silty mudstone and sandstone. The strata exposed at the foot of the mountains and in the trough valley are the Upper Permian Xuanwei Formation (P_3x), with gray-green, gray-yellow mudstone and siltstone interbedded with gray-black carbonaceous shale and coal seams. The dip direction is southeast, with an angle of 10°–20°. Structurally, it is located on the southeast wall of the Tuole hinge fault, which is nearly 200 m from the fault zone. This fault strikes 40° with a stratigraphic throw of around 40 m and is a compresso-shear fault. The southwest segment of the fault shows relative descent of the southeast wall, while the northeast segment shows relative uplift of the southeast wall. The main water-bearing rock formation in the study area is the Upper Permian Xuanwei Formation (P_3x), which consists of gray-green, gray-yellow mudstone and siltstone, with fissures as the main water-bearing medium, and moderate water abundance.

The groundwater recharge source is atmospheric precipitation. After infiltrating and recharging groundwater along well-developed fissures and joints, it flows from southeast to northwest. The survey area is located in the groundwater runoff zone, which is close to the fault zone, with well-developed fissures and joints; these fissures and joints provide relatively large groundwater

storage space (Figure 5).

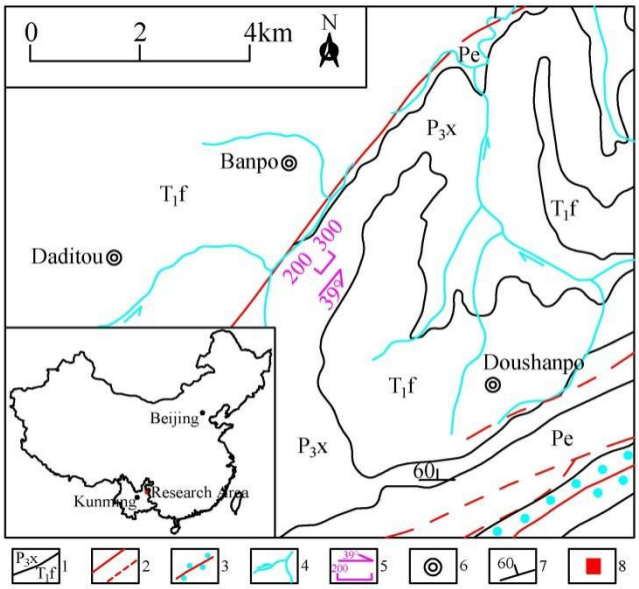


Fig. 5 Hydrogeological map of BaiaoVillage, Yunnan Province

1- stratum code and stratum boundary 2- measured fault and inferred fault 3- water-filled fault 4- river and flow direction 5- geophysical prospecting line and orientation 6- town and village location 7- stratum attitude 8- research area

3 Methodology

3.1 Exposed Type Areas

Based on the analysis of hydrogeological conditions, the groundwater in the study area is mainly conduit-type groundwater. Considering site conditions and drilling convenience, the geophysical survey line was laid out near the convergence point of two underground rivers, which is approximately perpendicular to the inferred direction of the underground rivers. The survey line orientation is 325°, with the starting station 1,070 m and the ending station 1,270 m (Figure 1).

356 The maximum elevation on the survey line is 1,370 m, the minimum elevation is 1,351 m, the
357 ground elevation at the window is 1,386 m, and the exposed groundwater level elevation is
358 1,331 m. Most of the survey line has limestone directly exposed at the surface, with high
359 resistivity, which meets the technical requirements for GPR. Therefore, GPR was selected for
360 groundwater detection. Field acquisition parameters are shown in Table 1.

361 **Table 1** Field set-up for GPR.

Equipment	PulseEKKO PRO produced by Canada Sensors & Software company
Frequency	25MHZ
Step Size	1m
Time Window	96,000ns
Survey Type	Reflection
Sampling Interval	3200ps
Antenna Separation	1 m
Antenna Polarization	Broadside
Antenna Orientation	Perpendicular

362

363 **3.2 Covered Type Areas**

364

365 **3.2.1 Thin Covered Type Areas**

366

367 Based on the analysis of hydrogeological conditions, the groundwater in the study area is mainly

karst fissure water. The aquifer is the medium-thick pure limestone of the Triassic Daye Formation (Td), with a single lithology and no carbonaceous or argillaceous content. According to preliminary geological data, the average thickness of the overburden in the study area is less than 10 m, and the site conditions are open. Based on these geological conditions, ERT was selected for water exploration. An east-west trending fault develops on the east side of the study area. Considering site conditions, the geophysical survey line was laid out approximately perpendicular to the east-west trending fault on the east side. The survey line orientation is 35°, with the starting station 100 m and the ending station 690 m (Figure 2). Field acquisition parameters are shown in Table 2.

Table 2 Field set-up for ERT.

Equipment	WGMD-3 (Chongqing Benteng Digital Control Technical Institute, China)
Array(electrode configuration)	Schlumberger (α 2) Array
Measuring point distance	10 m
Number of acquisition layers	20

3.2.2 Thick Covered Type Areas

Based on the analysis of hydrogeological conditions, the groundwater in the study area is mainly karst fissure water. The aquifer is the medium-thick pure limestone of the Lower Permian Maokou Formation (P_1m), with a single lithology and no carbonaceous or argillaceous content. According to preliminary hydrogeological surveys and collected drilling data from surrounding areas, the

385 average thickness of the overburden in the study area is greater than 40 m, which may reduce the
386 resolution of ERT for anomaly identification. The site conditions are open. Based on these
387 geological conditions, ERT and AMT were selected for comprehensive comparative groundwater
388 detection. Considering site conditions, the geophysical survey line was laid out along the
389 depression and approximately perpendicular to the strike of the strata. The survey line orientation
390 is 140°, with the starting station 200 m and the ending station 790 m (Figure 3). Field acquisition
391 parameters are shown in Tables 2–3.

392 **Table 3** Field set-up for AMT.

Equipment	EH-4 continuous conductivity profile instrument produced by American geometrics company
Orientation of electric field EX	140°
Orientation of magnetic field HY	230°
Measurement mode	Scalar
Working frequency	Low frequency band (10–1000 Hz), high frequency band (750–100000 Hz)
Measuring point distance	10 m

393

394 **3.3 Buried Type Areas**

395

396 **3.3.1 Shallow Buried Type Areas**

397

398 Based on the analysis of hydrogeological conditions, the groundwater in the study area is mainly

clastic rock fissure water. According to preliminary geological data, the water level in the study area is less than 10 m (shallow water level). The aquifer comprises the mudstone and sandstone of the Lower Triassic Feixianguan Formation (T_1f). Affected by water and lithology, a low-resistivity layer exists in the shallow part, which forms a good conductive shield for conventional resistivity methods. This conductive shield greatly reduces the exploration depth and resolution of conventional resistivity methods. The site conditions are open. Based on these geological conditions, the composite profiling method, ERT, and AMT were selected for comprehensive comparative detection. Considering site construction conditions, the geophysical survey line was laid out intersecting the northwest-southeast trending fault at a large angle. The survey line orientation is 318°, with the starting station 200 m and the ending station 495 m (Figure 4). Field acquisition parameters are shown in Tables 4–6.

Table 4 Field set-up for composite profiling method.

Equipment	WGMD-3 (Chongqing Benteng Digital Control Technical Institute, China)
Device	Rolling AMN and rolling MNB device
AO (distance from power supply electrode A to midpoint O of measuring electrode MN)	47.5m，62.5m，77.5m
BO (distance from power supply electrode B to midpoint O of measuring electrode MN)	47.5m，62.5m，77.5m
MN	5m
Point distance	5m

Table 5 Field set-up for ERT.

Equipment	WGMD-3 (Chongqing Benteng Digital Control Technical Institute, China)
Array(electrode configuration)	Schlumberger (α 2) Array
Measuring point distance	5 m
Number of acquisition layers	20

412 **Table 6** Field set-up for AMT.

Equipment	EH-4 continuous conductivity profile instrument produced by American geometrics company
Orientation of electric field EX	318°
Orientation of magnetic field HY	228°
Measurement mode	Scalar
Working frequency	Low frequency band (10–1000 Hz), high frequency band (750–100000 Hz)
Measuring point distance	10 m

413

414 **3.3.2 Deep Buried Type Areas**

415

416 Based on the analysis of hydrogeological conditions, the groundwater in the study area is mainly
417 clastic rock fissure water. According to preliminary geological data, the water level in the study
418 area is greater than 50 m (deep water level). The aquifer comprises the mudstone and siltstone of
419 the Upper Permian Xuanwei Formation (P_3x). The water level is deep, and the shallow resistivity
420 is relatively high compared with when water-bearing, which makes it suitable for conventional

electrical methods. However, the site is narrow. Therefore, AMT was first used for water exploration. Based on the AMT detection results, microtremor HVSR method was then used to further determine the drilling location. Considering site construction conditions, the geophysical survey line orientation is 39°, with the starting station 200 m and the ending station 300 m (Figure 5). Field acquisition parameters are shown in Tables 7–8.

Table 7 Field set-up for AMT.

Equipment	EH-4 continuous conductivity profile instrument produced by American geometrics company
Orientation of electric field EX	39°
Orientation of magnetic field HY	129°
Measurement mode	Scalar
Working frequency	Low frequency band (10–1000 Hz), high frequency band (750–100000 Hz)
Measuring point distance	10 m

Table 8 Field set-up for microtremor method.

Equipment	TROMINO (Italy)
Time window length	20 s
Sampling frequency	128 Hz
Acquisition time	25 min
Point distance	10 m, the abnormal section is encrypted to 5 m

4 Result analysis

430

431 **4.1 Exposed Type Areas**

432

433 The inversion result image obtained by GPR (Figure 6) depicts strong amplitude and chaotic
434 events in the reflection profile at stations 1,128–1,150 m at elevations 1,304–1,336 m and stations
435 1,184–1,200 m at elevations 1,305–1,330 m. Moreover, the site geology and underground river
436 development indicates that the section from stations 1,128–1,150 m at elevations 1,304–1,336 m is
437 a karst fracture zone, and the section from stations 1,184–1,200 m at elevations 1,305–1,330 m is
438 the location of a karst underground river conduit. Considering site construction conditions, the
439 borehole was finally placed at station 1,190 m.

440

441 Drilling data revealed a water-filled cave at elevations 1,313–1,324 m, which is a section of the
442 karst underground river conduit. The GPR method effectively identified the location and depth of
443 the karst underground river conduit. GPR can be effectively applied to groundwater exploration in
444 exposed type areas.

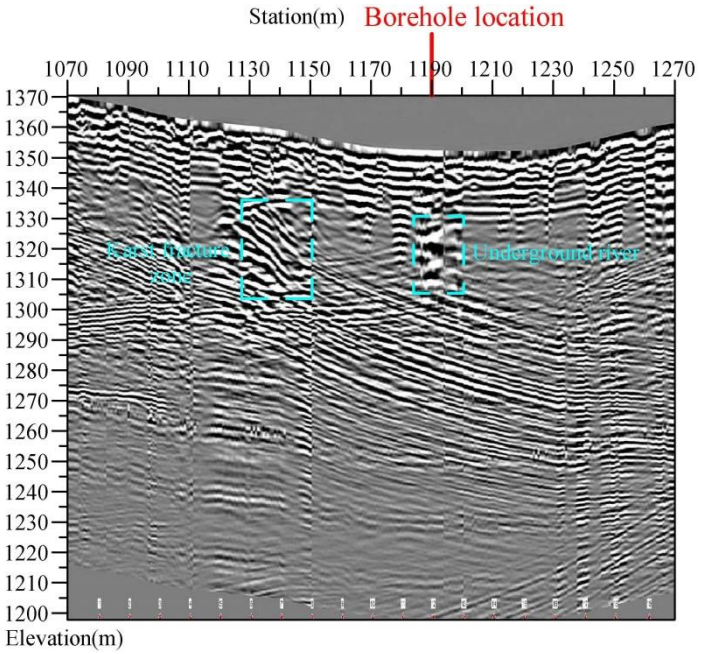


Fig.6 Ground Penetrating Radar (GPR) image map of Yibasan Village, Yunnan Province

4.2 Covered Type Areas

4.2.1 Thin Covered Type Areas

The apparent resistivity inversion contour section obtained by ERT (Figure 7) shows that the overburden resistivity ranges from 0 Ω·m to 300 Ω·m, with an average thickness of approximately 10 m, and a clear rock–soil interface. At stations 400–450 m, the resistivity is relatively lower than on both sides, and the resistivity contours show a “U”-shaped low-resistivity anomaly. Combined with the hydrogeological map and topography, this section is inferred to be a fault fracture zone. At stations 600–630 m, the resistivity contours show a low-resistivity anomaly extending obliquely downward toward the smaller station number direction, which is inferred to be a karst fracture zone. From the extension direction of the karst fracture zone, the karst and fault fracture

zones are found to be connected at a certain depth.

The exposed stratum in the study area is the Triassic Daye Formation (Td) aquifer. Influenced by the fault fracture zone at stations 400–500 m and the karst fracture zone at stations 600–630 m, groundwater converges and accumulates in the fault fracture zone. Considering site drilling conditions, the borehole was finally placed at the measurement point 455 m (edge of the fault fracture zone). Drilling verification showed that the water-bearing horizon in this borehole is the Triassic Daye Formation (Td), with an aquifer thickness of 55.8 m, a drawdown of 3.31 m, a yield of 4.767 l/s, and a specific yield of 1.44 l/s·m, which indicate moderate water abundance. The well depth is 122.5 m, and the well yield is 411.87 m³/d.

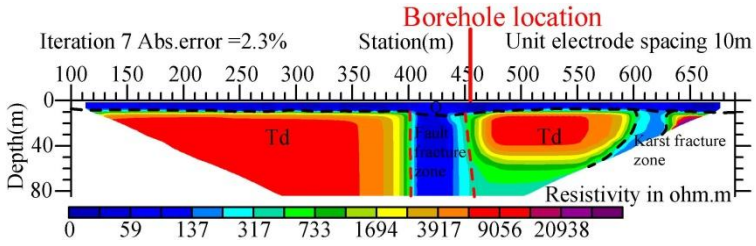


Fig.7 Contour profile of apparent resistivity inversion by the electrical resistivity tomography of Sanwan Village, Hunan Province

4.2.2 Thick Covered Type Areas

The apparent resistivity inversion contour section obtained by ERT (Figure 8a) illustrates that the entire profile is divided into three layers based on resistivity. In the shallow part of the 360–640 m measurement point section, gravel distribution (Q) exists, such that the shallow resistivity is

480 relatively high. The middle layer has low resistivity, which is inferred to be a clay layer
481 distribution area (Q). The bottom layer has relatively high resistivity, which is inferred to be the
482 bedrock distribution area ($P_1m + P_1q$). From the smaller to larger station numbers, the overburden
483 thickness gradually increases along the profile, with an average thickness of approximately 50 m,
484 and a clear rock–soil interface. Although the resistivity at stations 420–490 m shows a shallow
485 "U"-shaped low-resistivity distribution, its development depth is comparable to the overburden
486 thickness and cannot be interpreted as a karst fissure development zone. Therefore, due to the
487 thick overburden, the resolution of ERT for identifying karst fissures is reduced, which causes
488 difficulty in determining the borehole location. Therefore, AMT was combined for borehole
489 positioning. Based on the ERT results, AMT was used to detect groundwater in the 410–660 m
490 stations.
491
492 The AMT apparent resistivity inversion contour section (Figure 8b) reveals that the shallow part
493 has low resistivity, with an average thickness of around 50 m, which is inferred to be the
494 overburden (Q). Below 50 m, the resistivity is relatively high, which is inferred to be the bedrock
495 distribution area ($P_1m + P_1q$). A relatively low-resistivity anomaly exists at measurement points
496 445–510 m and depths of 50–135 m, which is inferred to be a karst fissure fracture zone.
497
498 Considering site drilling conditions, the borehole was finally placed at the measurement point
499 470 m. Drilling verification showed that the water-bearing horizon in this borehole is the Permian
500 Maokou-Qixia Formation ($P_1m + P_1q$). The exposed overburden thickness is 46.3 m. The main
501 water-bearing section is the dissolution fissures at 62.09–102.5 m. The borehole depth is 150 m,

the static water level is 10.5 m, and the well yield is 131.76 m³/d.

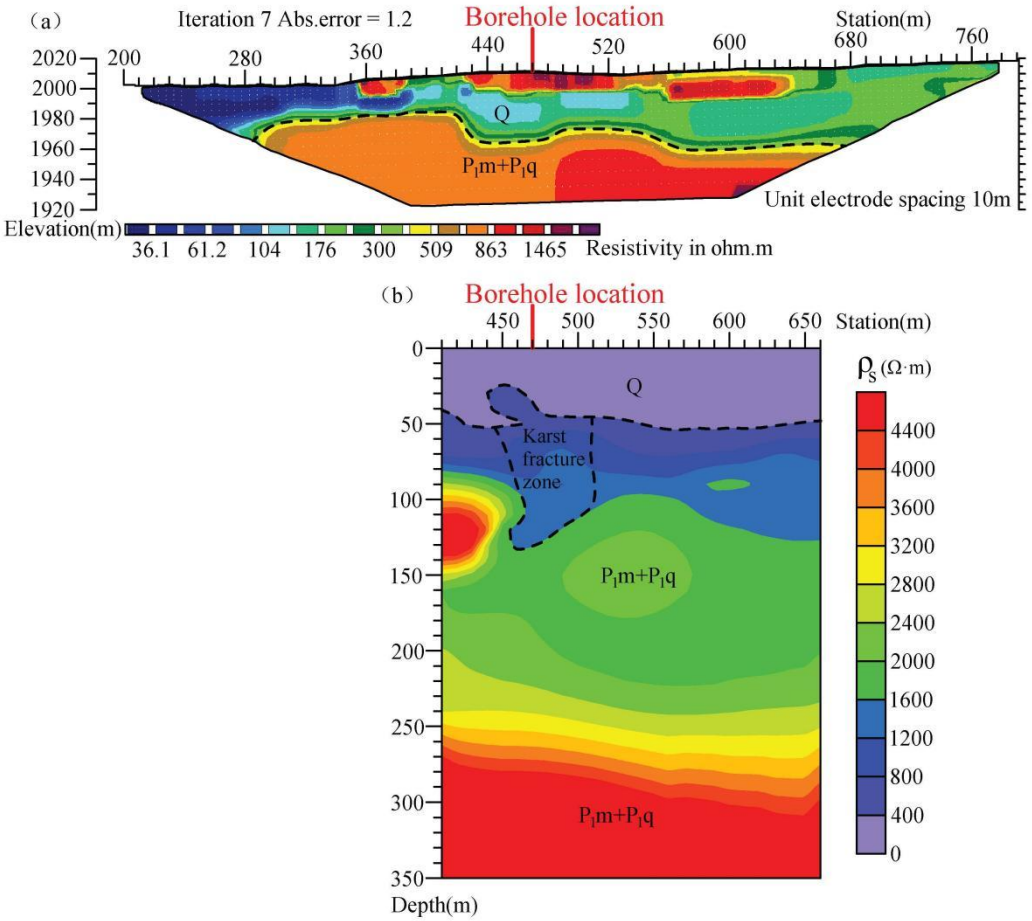


Fig.8 Integrated geophysical results profile plot of Hongdong Village, Yunnan Province

Fig.8a Contour profile of apparent resistivity inversion by the electrical resistivity tomography

Fig.8b Contour profile of apparent resistivity inversion by audio frequency magnetotelluric method

4.3 Buried Type Areas

4.3.1 Shallow Buried Type Areas

The apparent resistivity curve of the composite profiling method with different electrode spacings (Figure 9a) shows that the resistivity along the entire profile is relatively low, all less than

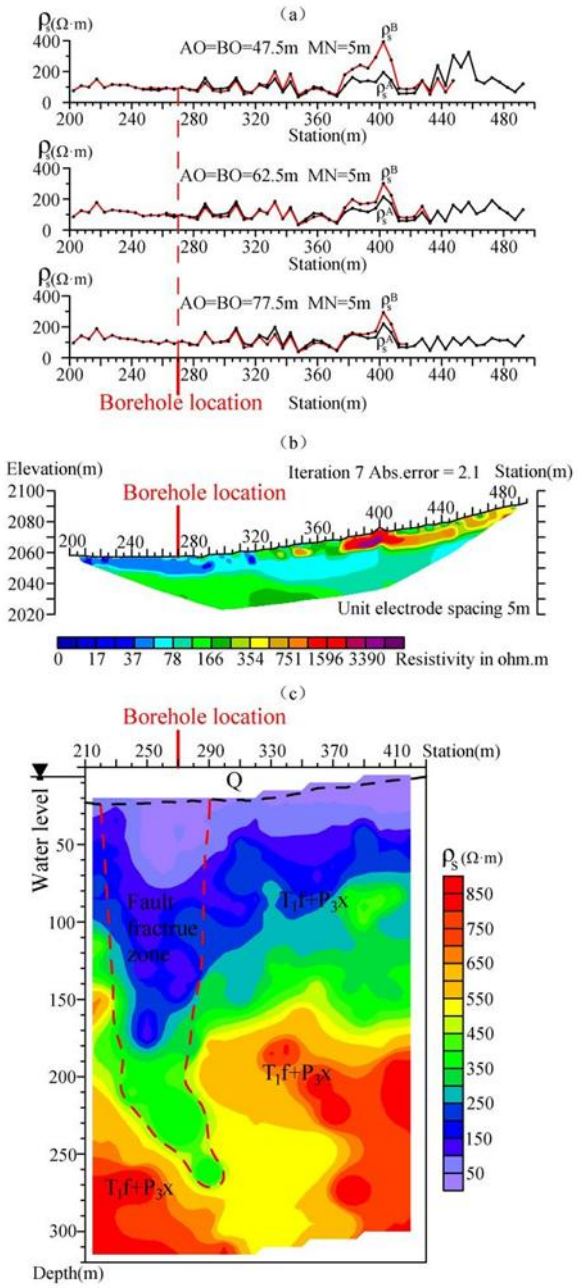
200 Ω·m, with a small range of variation. The resistivity varies significantly at local sections such as measurement points 400–410 m and 440–460 m, which is influenced by surface gravelly soil and gravel. The differentiation between the ρ_s^A and ρ_s^B curves of the composite profiling method is not obvious; the two curves essentially overlap, and the variation remains insignificant with increasing electrode spacing. The resistivity along the entire profile shows a jagged pattern, which causes difficulty in extracting useful anomaly information.

The apparent resistivity inversion contour section obtained by ERT (Figure 9b) depicts that the shallow part has large resistivity variations (0–4,000 Ω·m) and uneven resistivity distribution. After station 380 m, the resistivity increases sharply, which is due to the influence of surface gravel and gravelly soil. Ignoring the influence of surface gravel and gravelly soil, the resistivity along the entire profile is relatively low, all less than 200 Ω·m. Limited by site conditions, the survey line length and exploration depth are limited. Within the achievable exploration depth range, the apparent resistivity distribution is relatively uniform with a small variation range. Moreover, no obvious resistivity anomaly is observed in the survey area. These conditions cause difficulty in identifying effective anomalies such as fissures or fracture zones.

The apparent resistivity inversion contour section obtained by AMT (Figure 9c) reveals that the shallow part has low resistivity. Within a depth of 150 m, the resistivity is relatively low, which is less than 300 Ω·m. The resistivity along the entire profile is less than 900 Ω·m. Locally, relatively low-resistivity segments are found within the low-resistivity background. At stations 220–290 m at depths of approximately 10–190 m, a low-resistivity anomaly is observed. Combined with

hydrogeological data, a northwest-southeast trending fault develops near the survey line. Thus, this anomaly is inferred to be a fissure or fault fracture zone. At stations 230–270 m at depths of around 10–190 m, a relatively lower resistivity anomaly is found, which is inferred to be a water-rich zone.

Considering site drilling conditions, the borehole was finally placed at station 270 m, with a depth of 195 m. Drilling revealed that the aquifer is the Lower Triassic Feixianguan Formation (T_1f). Fissures developed at 92.4–93.8 m, which is the main water-producing section of the borehole. Fissures are relatively developed at 12.6–13.5 m, which is the secondary water-producing section of the borehole. Drilling revealed a static water level of 6.15 m, and a yield of 366.27 m^3/d at a drawdown of 31.44 m.



548

549 **Fig.9** Integrated geophysical results profile plot of Dalubian Village, Yunnan Province

550 Fig. 9a Apparent resistivity curve of composite profiling method

551 Fig.9b Contour profile of apparent resistivity inversion by the electrical resistivity tomography

552 Fig.9c Contour profile of apparent resistivity inversion by audio frequency magnetotelluric method

553

554 **4.3.2 Deep Buried Type Areas**

555

556 The apparent resistivity inversion contour section obtained by AMT (Figure 10a) shows that the
557 resistivity along the entire profile is relatively low, all less than 150 Ω·m. Locally, relatively
558 low-resistivity segments are found within the low-resistivity background. The resistivity changes
559 significantly around stations 225 and 265 m. Relatively low-resistivity anomalies exist at stations
560 215–225 m at depths of 30–70 m and at stations 265–300 m at depths of 30–150 m, which are
561 inferred to be fissure development sections (Figure 10a). Both of the abovementioned sections are
562 inferred to be water-rich sections.

563

564 The anomalies detected by AMT are broad in width, and two sets of anomalies are observed. In
565 addition, both anomalies are close to the boundaries of the survey line. To increase the success rate
566 of water production from the well, the microtremor HVSR method was used on the same survey
567 line for further determining the drilling location. The microtremor H/V ratio spectrum contour
568 map (Figure 10b) reveals that, at frequencies of 3.5–6.5 Hz and stations 272–285 m, 8–12 Hz and
569 stations 262–280 m, and 10–13 Hz and stations 235–245 m, high H/V ratio spectrum anomalies
570 are observed. These stations are inferred to be sections with good water-bearing capacity in karst
571 fissures.

572

573 Combining the anomalies from AMT and the microtremor HVSR method, as well as site
574 construction conditions, the borehole was finally placed at station 280 m. The borehole depth is
575 163.5 m. Drilling revealed that the aquifer is the mudstone and siltstone of the Upper Permian
576 Xuanwei Formation (P_3x). Fissures developed at 19.2–20.8 m, which is the main water-producing

section of the well. Fissures are relatively developed at 52.6–53.8 m and 75–78.8 m, which are secondary water-producing sections of the well. Drilling revealed a static water level of 50.07 m, and a yield of 181.44 m³/d at a drawdown of 1.61 m.

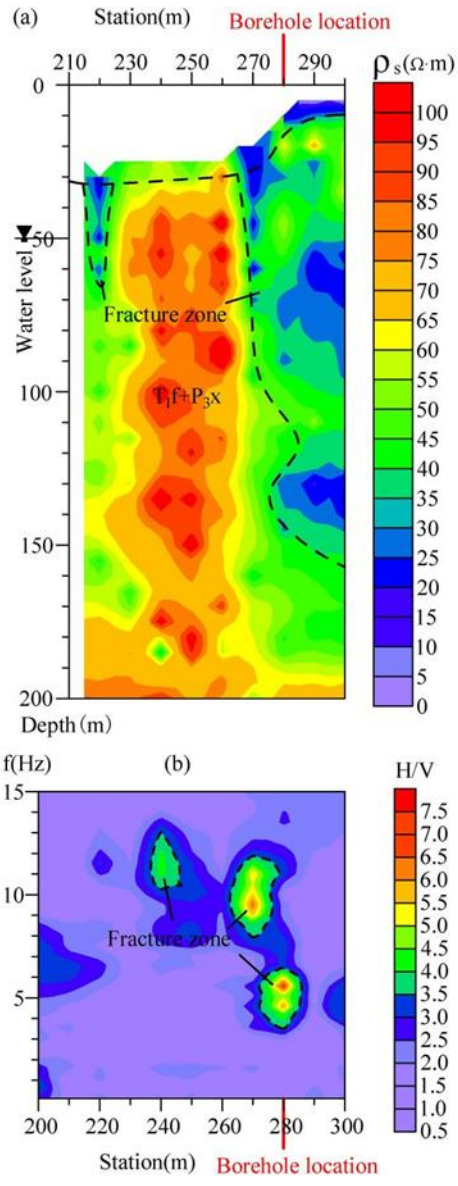


Fig.10 Integrated geophysical results profile plot of Baiao Village, Yunnan Province

Fig. 10a Contour profile of apparent resistivity inversion by audio frequency magnetotelluric method

Fig. 10b Contour map of the microtremor H/V ratio spectrum

5 Discussion

586 Unlike previous studies that focused solely on a single type of overburden or specific geophysical
587 methods, this paper systematically reviews the types of overburden and their hydrogeological
588 characteristics. It integrates the principles and applicability conditions of geophysical methods,
589 with an emphasis on analyzing their combinations and application cases in different overburden
590 areas, while also exploring optimization pathways for geophysical techniques. The novelty of this
591 work lies in being the first to propose differentiated sequences of geophysical techniques and
592 optimized combinations for the economical, rapid, and accurate detection of groundwater in
593 various types of overburden areas within the karst rocky mountain regions of Southwest China. In
594 doing so, it addresses the lack of systematic comparison and targeted technical construction in
595 previous research.
596 (1) Exposed type areas: When the target depth is shallow (less than 100 m), lower frequency
597 antennas (12.5 MHz) can be used to increase exploration depth. However, the unshielded nature of
598 low-frequency antennas limits the effective use of GPR in areas with severe electromagnetic
599 interference. When the target depth exceeds 100 m, TEM methods with greater exploration depth
600 should be selected. By analyzing the hydrogeological conditions of the study area and then
601 selecting favorable target areas for water exploration, the most economical, rapid, and effective
602 geophysical method is chosen. This method saves costs while improving the success rate of water
603 exploration.
604 (2) Thin covered type areas: When conducting water exploration in thin covered areas, if the karst
605 water-bearing rock formation is a relatively single lithology pure carbonate rock (without
606 carbonaceous or argillaceous rock) and the site is open and meets the exploration depth
607 requirements, then using only ERT can achieve good water exploration results. When the target

depth is large, the water-bearing rock formation is impure limestone, or the anomalies interpreted by ERT are broad, if any one of the three conditions is met, other methods should be combined for water exploration and well location.

(3) Thick covered type areas: When conducting water exploration in thick covered areas, affected by the thick overburden, the resolution of ERT for detecting karst fissures decreases. AMT, which has greater exploration depth and relatively better resolution, should be the primary method for detection. AMT has good water exploration results. However, when the anomalies interpreted by AMT inversion are broad and do not meet the requirements for well location, other methods should be considered for fine well positioning.

(4) Shallow buried type areas: When conducting water exploration in shallow buried areas, affected by the shallow water level and clastic rocks, a low-resistivity layer exists in the shallow part. This area forms a good conductive shield, which greatly reduces the exploration depth and resolution for karst fissures of the combined profiling method and ERT. AMT, which has greater exploration depth and relatively better resolution, should be the primary method for detection. AMT has good water exploration results in shallow buried areas. However, when the anomalies interpreted by AMT inversion are broad in range and do not meet the requirements for well location, other methods should be considered for fine well positioning.

(5) Deep buried type areas: When conducting water exploration in deep buried areas, the water level is deep, and the shallow resistivity is higher than the resistivity below the water level. When the site is open, conventional resistivity methods can be considered for water exploration. When the site is narrow, AMT can achieve good water exploration results. However, when the anomalies interpreted by AMT inversion are broad in range and multiple sets of anomalies are present, which

cause difficulty in meeting well location requirements, the microtremor HVSR method can be combined to further determine the well location.

In karst areas, the undulating topography and generally narrow site conditions affect the effectiveness of geophysical methods for groundwater exploration. In such areas, methods including ground penetrating radar (GPR), the transient electromagnetic method (TEM), and audio-frequency magnetotellurics (AMT) are susceptible to electromagnetic interference from high-voltage cables, which can generate false anomalies. The overburden in karst regions exhibits significant lateral thickness variations, making it difficult for the electrical resistivity tomography (ERT) method to simultaneously acquire shallow, intermediate, and deep data with a single electrode spacing. This results in less accurate imaging of the inversion model, causing deviations between inversion results and actual conditions. The audio-frequency magnetotellurics (AMT) and microtremor methods are considerably affected by field data acquisition procedures and the imaging performance of inversion software. Therefore, future research should proceed from both hardware and software perspectives. It is necessary to develop geophysical instruments with strong anti-interference capabilities and multi-parameter integration, design data processing software that integrates single or multiple parameters, achieve intelligent software processing, and establish three-dimensional data acquisition and processing systems.

6 Conclusions

The overburden has a decisive influence on geophysical groundwater detection. Based on different overburden types in the karst rocky mountain areas of Southwest China, the following rules for water exploration through drilling are summarized.

(1) Exposed type area: The soluble rock aquifer is directly exposed at the surface without continuous coverage of unconsolidated sediments. For exposed rocks such as limestone and dolomite, the resistivity is generally very high, which reaches $n\times10^4$–$n\times10^5$ Ω·m. In exposed type areas, the grounding condition is poor, the supply current is small, the measured voltage is high, and the measurement error is large. The surface electrical characteristics show high resistivity, which prevents current penetration and forms an insulating shield. This insulating shield reduces the exploration depth, which is unfavorable for the application of DC resistivity methods. However, for non-grounded electromagnetic methods, good application results can be achieved. When the detection depth is shallow, using low-frequency antenna GPR can achieve good water exploration results. When the detection depth is large, TEM methods are used. For groundwater detection in exposed type areas, geophysical methods often use non-grounded electromagnetic methods.

(2) Covered type area: The soluble rock aquifer is overlain by discontinuous layers of sediments such as clay, sand, and gravel. Given that the overburden generally contains clay, sand, or gravel, it forms an electrical layer with resistivities ranging from tens to hundreds of Ω·m. When the overburden is thin (less than 30 m), the overall surface resistivity is neither too high to prevent power supply nor too low to cause skin effect affecting exploration depth. Using conventional resistivity methods for groundwater detection can achieve good results. When the overburden is thick (greater than 30 m) or the site is narrow, on the one hand, arranging a long profile to achieve greater exploration depth is difficult; on the other hand, the resolution of resistivity methods for identifying karst fissure anomalies decreases. Therefore, under such conditions, electromagnetic methods (e.g., AMT, CSAMT, or TEM methods) are recommended.

(3) Buried type area: The soluble rock is overlain by clastic rocks. Common clastic overburden in the karst region of Southwest China mainly includes Jurassic and Cretaceous red beds (red silty rock, sandstone, locally interbedded with limestone fragments), Permian Emeishan basalt, and sandstone or shale from other formations. A clastic rock caprock of a certain thickness generally has its own independent groundwater level and no hydraulic connection with the underlying soluble rock. In this case, the clastic rock layer is the target aquifer for water exploration. The resistivity of this clastic rock layer is generally between tens and hundreds of Ω·m. For relatively intact, slightly weathered basalt, the resistivity can reach $n\times10^3$–$n\times10^4$ Ω·m. When the groundwater level is shallow, the surface clastic rocks are often completely to strongly weathered, with large voids, and are water-bearing or saturated, with low resistivity. This area forms a good conductive shield for conventional resistivity methods, which greatly reduces the exploration depth. As a result, conventional resistivity methods are generally unfavorable, and electromagnetic methods are recommended. When the groundwater level is deep, the shallow resistivity is relatively high. Depending on site conditions, conventional resistivity methods can be used within the target detection depth range. However, when site conditions are narrow and the target is deep, electromagnetic methods (AMT, CSAMT, or TEM methods) are recommended for groundwater detection.

(4) In the water exploration process for the different overburden types mentioned above, when geophysical anomalies are uncertain or ambiguous, other methods such as the microtremor HVSR method can be combined for comprehensive interpretation.

696 **References**

697 Alao JO, Abubakar F (2025) Groundwater exploration, management strategies and sustainability:
698 Geophysical approaches. Geosystems and Geoenvironment 4(3):100395 DOI：
699 10.1016/J.GEOGEO.2025.100395

700 Bon AF, Ombolo A, Biboum PM, Moutlen JM, Mboudou GE (2022) Identification of
701 hydrogeological features using remote sensing andelectromagnetic methods in the hard–
702 rock formations of the Cameroon coastal plain (Central Africa): Implications for water borehole
703 location. Scientific African 17: 2468−2276 DOI:10.1016/J.SCIAF.2022.E01272

704 Cao R, Ran Y, Lyu YX, Guo CD, Li DH, Wang Jia (2018) Application of geophysical prospecting
705 and hydrogeological analysis in borehole siting in the karst area: A case study of ZK3 well in
706 Luojiaba, Qianjiang district. Carsologica Sinica 37(2): 280-285 doi: 10.11932/karst20180215

707 Chen MX (1988) Some ecperiences in compiling hydrogeological maps of karstic terrains in
708 China. Carsologica Sinica 7(3): 199-203 doi:CNKI:SUN:ZGYR.0.1988-03-006

709 Fokker E, Carpentier S (2024) Complementary geophysical methods for monitoring groundwater
710 pressure and saturation, Netherlands Journal of Geosciences 103(26): e26
711 DOI:10.1017/njg.2024.23

712 Gabriel EO, Sodiq BA, Taofeeq AI, Yusuf M, Kayode AO, Jimoh A, Saminu O, Oluwafemi AO,
713 Ojulari BA (2025) Geophysical investigation of groundwater potential and aquifer properties
714 using ground magnetic and vertical electrical sounding at the University of Ilorin, Nigeria.
715 Modeling Earth Systems and Environment 11(3) :205 DOI:10.1007/S40808-025-02383-2

716 Guo LL, Wei LS, Huang AB, Shu QF (2022) Structure of karst groundwater system and its water
717 exploration in Wumeng Mountain area. Bulletin of Geological Science and Technology 41(1):

146-156, 167 doi: 10.19509/j.cnki.dzkq.2022.0025

Huang LS, Hou YJ, Chen YR, Jing RZ, Wang JC, Zhao Y, Li XB, Pei C, Zeng YQ, Zeng H (2022) Rapid and accurate positioning concealed fault using geophysical and geochemical techniques in cities and surrounding areas: A case study of Lingui District, Guilin City, Guangxi. Geology in China 49(3):929−942 DOI:10.2029/gc20220317

Laskow M, Gendler M, Goldberg I, Gvirtzman H, Frumkin A (2011) Deep confined karst detection, analysis and paleo-hydrology reconstruction at a basin-wide scale using new geophysical interpretation of borehole logs. Journal of Hydrology 406(3-4):158-169 DOI：10.1016/j.jhydrol.2011.06.011

Li W, Tang CR, Wei LS, Shu QF, Tao JL, TianYC, Chen CL, Luo B (2022) Application of various geophysical prospecting method in red beds water exploration. Computing Techniques for Geophysical and Geochemical Exploration 44(3): 353−360 GB/T 7714-2015

Liang DH, Gan FP, Zhang W, Han K (2020) Study on the effectiveness of the microtremor HVSR method in detecting underground river pipelines and caves in karst areas. Carsologica Sinica 39(1): 95-100 doi: 10.11932/karst20200104

Liao WP, Zhu T, Huang RH, Zhang ZL (2017) The application of comprehensive geophysical prospecting method in water exploration. Computing Techniques for Geophysical and Geochemical Exploration 9(6): 768−774 DOI: 10.3969/j.issn.1001-1749.2017.06.09

Liu JY, Gao YX, Wang J, Zhu TY, Ding PB, Zhou GG, Li SJ (2024) Seismoelectric Imaging of Aquifer Interface: Theoretical Investigation and Laboratory Experiments. Geophysical Research Letters 51(23) DOI: 10.1029/2024GL112534

740 Liu W, Gan FP, Zhou QY, Zhang W (2019) Probing geological conditions of karst collapses using
741 high -density resistivity imaging and microtremor spectral ratio methods: an example of Langxia
742 village, Jiaotang town, Gaoyao City, Guangdong Province. Geol Exploration 55(1):115–126
743 DOI:cnki:sun:dzkt.0.2019-01-012
744 Pan XD, Zhang FW, Meng XJ, Zeng J, Chen ZB (2015) Model for Groundwater Searching with
745 Drilling in Karst Area near Deep Valley. Geoscience 29(2):272-278
746 DOI:10.3969/j.issn.1000-8527.2015.02.008
747 Pei JG, Liang MZ, Chen Z (2008) Classification of karst groundwater system and statistics of the
748 main characteristic values in Southwest China karst mountain. Carsologica Sinica 27(1): 6-10 doi:
749 10.3969/j.issn.1001-4810.2008.01.002
750 Qi X, Li QH, Zhang ZT, Wang XH, Dai T (2021) Electrical characteristics and storage rules of
751 groundwater in granite area of Qiongzhong County Hainan Province. Geological Bulletin of China,
752 40(6): 1001-1009 DOI: 10.12097/gbc.dztb-40-6-1001
753 Rulff P, Castillo-Reyes O, Koyan P, Martin T, Deleersnyder W, Mascarell MC (2025)
754 Geoelectrical and electromagnetic imaging methods applied to groundwater systems: recent
755 advances and future potentials, EGU General Assembly DOI:10.5194/egusphere-egu24-65
756 Subramani D, Kamaraj P, Abd E (2024) Groundwater Exploration for Sustainable Development
757 and Management in a Hard Rock Basin. Applied and Environmental Soil Science DOI：
758 10.1155/2024/7769047
759 Sun SY, Zhang JZ (2025) Application of seismoelectric fusion in deep groundwater exploration.
760 Urban Geology 20(2):229-234 GB/T 7714-2015
761 Sun YH, Lian J, Wu Y (2012) Geophysical prospecting techniques in discriminating the in filled

762 water from mud in karst water-bearing media. Carsologica Sinica 31(4):459-464 doi:
763 10.3969/j.issn.1001-4810.2012.04.016
764 Wang DJ, Qian JZ, Ma L, Xu HM, Wang XY, Wang YY (2022) Integration of multiple
765 hydrogeological survey technologies for exploring the groundwater distribution in karst areas: A
766 case study in Xingfu Spring, Chaohu City, China. Journal of Hydrology 614 (pb) DOI：
767 10.1016/J.JHYDROL.2022.128637
768 Wang WJ，Zheng MY (2021) Vertical zoning characteristics of water storage tectonic units in
769 dolomite outlying area on slope of Guizhou Plateau — A case study of water storage units in slope
770 area of Chishui River Basin. Groundwater 43(2):24-26 GB/T 7714-2015
771 Wang Y (2002) Classification,features of karst water system and key point for the evaluation to
772 karst water exploration in southwest china karst area. Carsologica Sinica 21(2):114-119 doi:
773 10.3969/j.issn.1001-4810.2002.02.008
774 WangY (2003) Classification of karst water systems in karst down-faulted basins of the
775 southwestern China karst region. Geology in china 30(2): 220-224 DOI: 10.12029/gc20030217
776 Wang YF, Xue GQ, Han JT, Luo XZ, Wang BB, Ge C, Xu H, Guan HC, Wang QS, Zhang K,
777 Wang C, Zhang XR, Tao W, Zhang JZ, Liu XH (2025) Progress in geophysical exploration of
778 groundwater and its technical innovation. Geology in China 52(4): 1325−1351 DOI：
779 10.12029/gc20240610001
780 Zheng ZJ, Liu W, Zeng J, Gan FP, Lu XH (2024) An integrated geophysical approach for ground
781 water prospecting in plateau slope zone: a case study from Shuangnuo Village, Fuyuan, Yunnan
782 Province. Environmental Earth Sciences 83(6) DOI:10.1007/S12665-024-11452-1
783 Zheng ZJ, Yan JY, Zeng J, Gan FP, Liu W, Lu XH (2025) Integrated geophysical methods for

784 ground water prospecting in fault fracture zones under low-resistivity background conditions: a
785 case study from Laohutiangou Village, Xuanwei, Yunnan Province. Earth Science Informatics, 18
786 (2):209 DOI:10.1007/S12145-025-01717-Z
787 Zheng ZJ, Zeng J, Zhao W, Gan FP (2019) Application research of high density resistivity method
788 in water exploring in karst area. Progress in Geophysics 34(3):1262-1267 DOI：
789 10.6038/pg2019CC0190
790 Zohdy A A R, Eaton G , Mabey D R (1974) Application of surface geophysics to ground-water
791 investigations. Techniques of Water-Resource Investigation DOI:10.3133/twri02d1

Groundwater Detection Using Geophysical Methods in Different Overburden Types in the Karst Region of Southwest China

Zhijie Zheng [1, 2, 3], Jie Zeng [1, 3], Jiayong Yan[4*], Fuping Gan [1, 3], Xiuhua Lu [1, 3]

1. Institute of Karst Geology, Chinese Academy of Geological Sciences /Key Laboratory of Karst Dynamics, MNR & GZAR/International Research Center on Karst under the Auspices of UNESCO, Guilin, Guangxi, China；2. School of Resources and Environmental Engineering, Hefei University of Technology, Hefei, Anhui, China；3. Pingguo Guangxi, Karst Ecosystem, National Observation and Research Station, Pingguo, Guangxi, China; 4. SinoProbe Laboratory，Chinese Academy of Geological Sciences , Beijing, China

*Corresponding author: Jie Zeng , Email: 522594381@qq.com

Declarations

Ethics approval and consent to participate: This study was approved by Institute of Karst Geology, School of Resources and Environmental Engineering, Hefei University of Technology, Pingguo Guangxi, Karst Ecosystem, National Observation and Research Station and SinoProbe Laboratory.

Consent for publication: This is to confirm that the manuscript titled " Groundwater Detection Using Geophysical Methods in Different Overburden Types in the Karst Region of Southwest China" has never been published before. Also, it is not currently being considered for publication in any other journal.All the listed authors have carefully reviewed and approved this manuscript. We all agree to submit it to Hydrogeology Journal for publication and accept the journal's publication policies.

Availability of data and materials: The data that support the findings of this study are available on request from the corresponding author, upon reasonable request.

Competing interests: The authors declare no competing interests.

Funding： Regional Geological Survey of the Du'an-Heshan Area in Central Guangxi (DD202501029), Regional Geological Survey of the Hechi Area in North Guangxi(DD20240102404).

Authors' contributions: Zhijie Zheng and Jie Zeng wrote the main manuscript text, Jiayong Yan checks the quality of article, Fuping Gan prepared fgures 1-5. Xiuhua Lu prepared fgures 6–10. All authors reviewed the manuscript.

Acknowledgements: The authors thank Wei Liu and Wei Zhao for the helpful suggestions. We extend sincere

*Corresponding author: Jie Zeng , Email: 522594381@qq.com

819 gratitude to the editors and the anonymous reviews for the valuable advice on how to improve this manuscript.

820 **Corresponding author:** Jie Zeng , Email: 522594381@qq.com